

Joint Subcarrier Assignment and Power Allocation for OFDMA Full Duplex Distributed Antenna Systems

Zhan Liu, Suili Feng, *Member, IEEE*

Abstract—In this paper, we investigate the resource allocation scheme for orthogonal frequency division multiple access (OFDMA) full-duplex (FD) distributed antenna systems (DASs), in which both remote access units (RAUs) and users having the full-duplex capability. We aim to maximize the system spectral efficiency through jointly optimizing subcarrier assignment and power allocation, where users' uplink/downlink quality of service requirements, per-user uplink/downlink transmit power constraints, and subcarrier reuse are considered. The user-centric virtual cell approach is adopted to reduce the computational and signaling overhead. Based on the successive convex approximation method and penalty factor, we propose an efficient overall optimization algorithm to tackle the non-convex optimization problem. Simulation results show that the proposed algorithm can achieve performance close to the exhaustive search algorithm, comparable to the hierarchical decomposition algorithm using the optimal subcarrier allocation scheme, and better than other benchmark algorithms. In addition, the proposed algorithm can guarantee fairness among users at a low cost of system spectral efficiency.

Index Terms—Orthogonal frequency division multiple access (OFDMA), full-duplex (FD), distributed antenna system (DAS), spectral efficiency, resource allocation.

I. INTRODUCTION

FUTURE wireless communication systems need to provide ubiquitous network coverage and high data rates to meet the growing demand for wireless services. These demands require more reasonable and effective use of current spectrum resources [1], [2]. Among the physical layer technologies, distributed antenna systems (DASs), also called cloud radio access networks (C-RANs), can shorten the access distance between users and remote access units (RAUs) and the consequent reducing transmission power and reducing path loss, which can effectively reduce interference and improve system capacity. However, most studies on DASs only consider the uplink [3], [4] or the downlink [5], [6], all of them have some limitations for achieving high spectrum resource utilization. On the other hand, full-duplex (FD) technology can simultaneously perform uplink and downlink transmission at the same

frequency, which is capable of achieving double the capacity of half-duplex (HD) technology theoretically [7]. However, compared with an HD network, the newly added interference, especially the self-interference from the transmitters to itself, restricts FD technology development. Fortunately, the advent of many advanced self-interference cancellation technologies [8]–[10] makes FD operation feasible, which has been widely adopted in various network scenarios [11], [12]. Moreover, the combination of FD technology and DASs to form FD-DASs is considered to complement each other, which has attracted considerable attention [13], [14]. [15] showed that by using advanced interference cancellation strategies, FD C-RAN can achieve higher spectral efficiency than HD C-RAN. [16] revealed that power allocation and hybrid FD/HD operation can improve the performance of C-RAN. It should be noted that these researches considered narrowband communications, and all RAUs and users are in the same spectrum.

Due to the fact that it can effectively combat frequency selective fading and improve spectral efficiency, orthogonal frequency division multiple access (OFDMA) has been widely adopted in FD systems [17]–[22] or HD DASs [23]–[27]. In [17], a joint uplink and downlink user pairing, subchannel assignment, and power allocation problem to maximize the sum-rate for an OFDMA FD single-input single-output (SISO) system was investigated. The authors first proposed a suboptimal matching algorithm to solve the user-pairing and subchannel allocation problem and then utilized the water-filling algorithms to solve the downlink power allocation and uplink power allocation, respectively. A similar problem was investigated in [18], the author proposed an iterative two-step solution algorithm for the joint problem; the first step was joint user pairing and subcarrier allocation based on a defined signal-to-noise ratio (SNR) threshold. The second step was to use the alternating direction method of the multiplier to solve the uplink and downlink power allocation problems, respectively. A resource allocation algorithm was considered in [19] to maximize the sum-rate performance by jointly optimizing subcarrier assignment and power allocation in FD OFDMA SISO networks. The authors developed a solution that blends iterative subcarrier assignment and water-filling power allocation. In [20], the authors investigated joint subcarrier scheduling and power allocation methods to maximize the uplink sum-rate in wireless powered communication networks for FD OFDM SISO systems, where employ wireless information transmission in the uplink and wireless energy transmission in the downlink. However, the studies in [17]–

Copyright (c) 2015 IEEE. Personal use of this material is permitted. However, permission to use this material for any other purposes must be obtained from the IEEE by sending a request to pubs-permissions@ieee.org.

Z. Liu is with School of Electronic and Information Engineering, South China University of Technology, Guangzhou 510641, China, and with the Department of Information Science and Engineering, Hunan University of Humanities, Science and Technology, Loudi 417000, China (e-mail: delabe@163.com).

S. Feng is with School of Electronic and Information Engineering, South China University of Technology, Guangzhou 510641, China (e-mail: fengsl@scut.edu.cn).

[20] did not consider the users' quality of service (QoS) requirements. In [21], the subcarrier assignment and power control were jointly considered to maximize the energy efficiency for FD OFDMA SISO networks. A penalty function was introduced to handle the binary subcarrier assignment variables, then the authors proposed a two-layer iterative algorithm to obtain the locally optimal solution of the problem. In [22], the authors developed a framework to maximize the energy efficiency by optimizing joint user-RAU association, subchannel assignment, and power control considering FD OFDMA small cell, but each user can only connect to one RAU. In [23], the authors investigated the power allocation scheme for a downlink OFDM DAS system under both total and individual power constraints. In [24], the authors proposed joint power control and fronthaul rate allocation optimization to maximize the throughput performance of an OFDMA-based downlink C-RAN system. The authors of [25] developed three power allocation schemes for downlink OFDM DAS subject to the per-antenna maximum power constraints. In [26], the authors developed energy-efficient resource allocation with proportional fairness for downlink multiuser OFDM DAS. In [27], the authors proposed an energy-efficient scheme of joint antenna-subcarrier-power allocation for min-rate guaranteed services in the downlink multiuser OFDM DAS with limited backhaul capacity. Note that in the above works [23]–[27], only either uplink or downlink transmission was considered. To take a step further, the authors investigated joint uplink and downlink transmissions in [28] to maximize the system throughput in OFDMA C-RAN, but only HD capability was considered in all nodes. Recently, OFDMA technology has also been applied in FD DAS. In [29], the authors considered the downlink transmission of the FD DAS with energy recycling and proposed joint downlink power control and subcarrier assignment optimization to maximize the energy efficiency, where RAUs were operating in FD mode but can only transmit information in the downlink and recycle energy in the uplink simultaneously. As well, most of the above papers did not consider subcarrier reuse. In fact, if an appropriate resource allocation strategy is adopted, the potential performance of subcarrier reuse will be higher than that of the exclusive subcarrier assignment [27], [30], [31]. Moreover, the above researches considered the joint processing of all RAUs, which will incur heavy computational and signaling overhead, especially in the case of dense networks.

In this paper, we investigate the resource allocation problem in an OFDMA DAS with FD-capable RAUs and users. In particular, we jointly optimize the uplink/downlink power allocation and subcarrier assignment for maximizing spectral efficiency. The constraints of per-user uplink/downlink quality of service (QoS) requirements, subcarrier reuse, per-user uplink/downlink transmit power constraints are considered. To the best of our knowledge, this problem is practical but has not been investigated in the existing literature. On the other hand, multi-RAU design, FD operation, and subcarrier reuse also make the problem more complicated. To reduce the computational and signaling overhead, we take advantage of the distributed placement of RAUs in DAS and adopt the user-centric approach [6], [32]. In particular, each user selects

a nearby group of RAUs to form its virtual cell, and each user can only be served by its virtual cell. Therefore, compared to processing all RAUs jointly, the number of channels that need to be measured and the number of variables that need to be calculated become small. Inspired by [21], [33], an efficient overall algorithm is proposed for joint power allocation and subcarrier assignment based on the successive convex approximation method and penalty factor. The convergence of the proposed algorithm is proved. Simulation results illustrate the effectiveness of our proposed algorithm and demonstrate its superiority compared with other benchmark schemes. The main contributions of this paper are summarized as follows:

- We study the spectral efficiency maximization problem in an OFDMA-based FD DAS under the constraints of users' QoS requirements, per-user uplink/downlink transmit power, and subcarrier reuse. This problem is practical but has not been investigated in the existing literature to the best of our knowledge.
- We extend the concept of the user-centric virtual cell to our scheme to reduce the computational and signaling overhead, in which each user chooses a few neighboring RAUs to form its virtual cell and can only be served by its virtual cell.
- A non-convex mixed-integer nonlinear programming (MINLP) optimization problem is formulated for maximizing the system spectral efficiency, which is NP-hard and intractable. We propose an efficient overall optimization algorithm to obtain a suboptimal solution by exploiting the successive convex approximation method and penalty factor.
- Simulation results show that the performance of the algorithm is close to the exhaustive search algorithm and comparable to the hierarchical decomposition algorithm using the optimal subcarrier assignment scheme, but the complexity of our proposed algorithm is lower than that of the two benchmark algorithms. Moreover, our proposed algorithm significantly outperforms other benchmark schemes. Additionally, our proposed algorithm can guarantee fairness among users while having little impact on system spectral efficiency.

The rest of this paper is organized as follows. In Section II, we present the system model and formulate the optimization problem. We reformulate the spectral efficiency problem and describe the proposed algorithm in Section III. In Section IV, simulation results are presented to evaluate the performance of the proposed algorithm. Finally, conclusions are drawn in Section V.

Notations: Boldface capital and lowercase letters represent matrices and vectors, respectively; \mathbf{A}^H is the Hermitian transpose of \mathbf{A} ; $\text{Tr}(\mathbf{A})$ is the trace of \mathbf{A} and $\binom{n}{m} = \frac{n!}{m!(n-m)!}$ is the binomial coefficient; \mathbf{I}_N denotes an $N \times N$ identity matrix; $x \sim \mathcal{CN}(\mu, \sigma^2)$ is a complex Gaussian distribution with mean μ and variance σ^2 ; $E[\cdot]$ denotes the expectation operator; $\text{diag}\{x_1, \dots, x_n\}$ is the diagonal matrix composed by x_1, \dots, x_n ; $\mathbb{C}^{N \times M}$ denotes the set of $N \times M$ complex matrices; $\det(\cdot)$ represents the determinant operator.

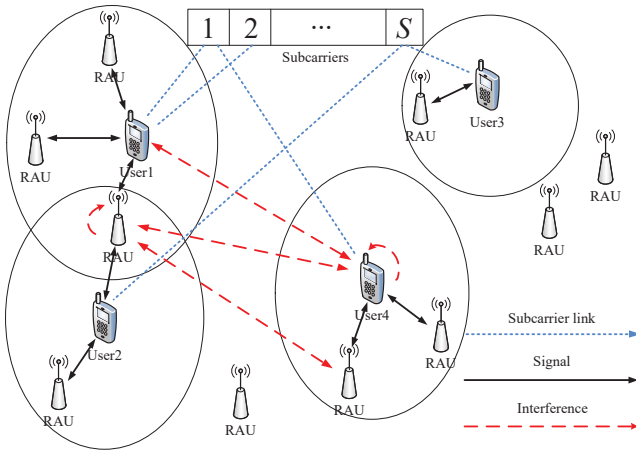


Fig. 1. System model with $N = 10$ RAUs, $K = 4$ users, $V_1 = 3$, $V_2 = 2$, $V_3 = 1$, and $V_4 = 2$.

II. SYSTEM MODEL AND PROBLEM FORMULATION

A. System Model

We consider a multiuser OFDMA-based FD DAS, which consists of S perfectly orthogonal subcarriers, N single-antenna RAUs, and K single-antenna users; both RAUs and users having FD capability¹, as depicted in Fig. 1. Denote the set of subcarriers, RAUs, and users as $\mathcal{S} = \{1, \dots, S\}$, $\mathcal{N} = \{1, \dots, N\}$, and $\mathcal{K} = \{1, \dots, K\}$, respectively. We assume that each RAU is connected to the baseband unit (BBU) by coaxial or optical fiber, and the signals can be centrally processed by the BBU². We assume that perfect channel state information (CSI) is available at the BBU. Specifically, the downlink CSI can be estimated at the users through the broadcast pilot signal sent by the BBU and then feedback to the BBU, and the BBU estimates the uplink CSI by receiving the access signal sent by the users. In FD DAS, only a few nearby RAUs will significantly contribute to a user due to path loss. To reduce the computational and signaling overhead, we adopt the user-centric virtual cell approach in which each user selects a nearby group of RAUs to form its virtual cell and can only be served by its virtual cell. Let \mathcal{V}_i be the virtual cell for serving user i with $|\mathcal{V}_i| = V_i$ for all $i \in \mathcal{K}$. We assume subcarrier reuse, each user can be served by multiple subcarriers, and each subcarrier can be allocated to multiple users.

In this paper, we consider the composite fading channel, let $\mathbf{h}_{\mathcal{V}_i, i, s} \in \mathbb{C}^{V_i \times 1}$ denote the channel vector from user i to virtual cell \mathcal{V}_i on subcarrier s , which can be modeled as

$$\mathbf{h}_{\mathcal{V}_i, i, s} = \sqrt{(d_{\mathcal{V}_i, i})^{-\gamma}} \circ \boldsymbol{\alpha}_{\mathcal{V}_i, i, s} \circ \mathbf{w}_{\mathcal{V}_i, i, s}, \quad (1)$$

where \circ is Hadamard product, $d_{\mathcal{V}_i, i} \in \mathbb{C}^{V_i \times 1}$ represents the distance vector between user i and virtual cell \mathcal{V}_i , γ is the path

¹A single antenna can cancel the self-interference to the receiver noise floor by adopting analog and digital cancellation techniques, so as to ensure that there is no degradation to the received signal, and can simultaneously transmit and receive on the same channel [9].

²Our considered system can be interpreted as a macroscopic multiple-antenna system. The downlink is the multiple-input single-output (MISO) channel, and the uplink is the single-input multiple-output (SIMO) channel.

loss factor, $\boldsymbol{\alpha}_{\mathcal{V}_i, i, s} \in \mathbb{C}^{V_i \times 1}$ denotes the lognormal shadow fading vector, $\mathbf{w}_{\mathcal{V}_i, i, s} \in \mathbb{C}^{V_i \times 1}$ represents the small-scale fading vector which follow the independent and identically distributed (i.i.d) Gaussian distribution with zero mean and unit variance. The composite channel from virtual cell \mathcal{V}_i to user i and from user i to user k are all generated in the same way. Define subcarrier allocation indicator $z_{i, s} \in \{0, 1\}$, where $z_{i, s} = 1$ if subcarrier s is assigned to user i , and $z_{i, s} = 0$ otherwise.

The uplink received signal from user i on subcarrier s can be written as

$$\mathbf{y}_{i, s}^U = \underbrace{z_{i, s} \mathbf{h}_{\mathcal{V}_i, i, s} x_{i, s}^U}_{\text{desired signal}} + \underbrace{\sum_{k \in \mathcal{K}, k \neq i} z_{k, s} \mathbf{h}_{\mathcal{V}_i, k, s} x_{k, s}^U}_{\text{user-to-RAU interference}} + \underbrace{\sum_{j \in \mathcal{K}} z_{j, s} \mathbf{H}_{\text{SI}, s} \mathbf{x}_{j, \mathcal{V}_j, s}^D}_{\text{RAU-to-RAU interference}} + \mathbf{n}_{i, s}^U, \quad (2)$$

where $x_{i, s}^U$ represents the transmitted signal from user i on subcarrier s with $E[|x_{i, s}^U|^2] = q_{i, s}$, $\mathbf{x}_{j, \mathcal{V}_j, s}^D \in \mathbb{C}^{V_j \times 1}$ denotes the transmitted signal vector from the virtual cell \mathcal{V}_j to user j on subcarrier s with diagonal power loading matrix as

$$E[\mathbf{x}_{j, \mathcal{V}_j, s}^D (\mathbf{x}_{j, \mathcal{V}_j, s}^D)^H] = \mathbf{P}_{j, s} = \text{diag}\{p_{j, 1, s}, \dots, p_{j, V_j, s}\}, \quad (3)$$

$\mathbf{n}_{i, s}^U \sim \mathcal{CN}(0, \sigma^2 \mathbf{I}_{V_i})$ represents the additive white Gaussian noise (AWGN), $\mathbf{H}_{\text{SI}, s} \in \mathbb{C}^{V_i \times V_j}$ denotes the residual self-interference matrix from virtual cell \mathcal{V}_j to virtual cell \mathcal{V}_i on subcarrier s . We treat the residual self-interference as noise and model it as $\mathbf{H}_{\text{SI}, s} = \sqrt{\sigma_{\text{SI}}^2} \sqrt{(d_{\mathcal{V}_i, \mathcal{V}_j})^{-\gamma}} \circ \boldsymbol{\alpha}_{\mathcal{V}_i, \mathcal{V}_j, s} \circ \left(\sqrt{\frac{a}{a+1}} + \sqrt{\frac{1}{a+1}} \mathbf{w}_{\mathcal{V}_i, \mathcal{V}_j, s}\right) \circ e^{j\theta}$ [34], σ_{SI}^2 is the self-interference cancellation level, a denotes the Rician factor, and the phase coefficient of θ is uniformly distributed in $[0, 2\pi]$. The achievable spectral efficiency of user i in the uplink is given by

$$R_i^U(\mathbf{P}, \mathbf{q}, \mathbf{z}) = \sum_{s \in \mathcal{S}} \log \det \left(\mathbf{I}_{V_i} + \frac{z_{i, s} q_{i, s} \mathbf{h}_{\mathcal{V}_i, i, s} \mathbf{h}_{\mathcal{V}_i, i, s}^H}{\Phi_{i, s}^U} \right), \quad (4)$$

where $\mathbf{P} = [\mathbf{P}_{1, 1}, \mathbf{P}_{1, 2}, \dots, \mathbf{P}_{K, S}]$ denotes the set of downlink power allocation, $\mathbf{q} = [q_{1, 1}, q_{1, 2}, \dots, q_{K, S}]$ is the uplink power allocation vector, $\mathbf{z} = [z_{1, 1}, z_{1, 2}, \dots, z_{K, S}]$ represents the subcarrier assignment of all users, and $\Phi_{i, s}^U$ is the interference-plus-noise of user i on subcarrier s in the uplink transmission, which can be expressed as

$$\Phi_{i, s}^U = \sum_{k \in \mathcal{K}, k \neq i} z_{k, s} q_{k, s} \mathbf{h}_{\mathcal{V}_i, k, s} \mathbf{h}_{\mathcal{V}_i, k, s}^H + \sum_{j \in \mathcal{K}} z_{j, s} \mathbf{H}_{\text{SI}, s} \mathbf{P}_{j, s} \mathbf{H}_{\text{SI}, s}^H + \sigma^2 \mathbf{I}_{V_i}. \quad (5)$$

The downlink received signal of user i on subcarrier s can

be written as

$$y_{i,s}^D = \underbrace{z_{i,s} \mathbf{h}_{i,\mathcal{V}_i,s}^H \mathbf{x}_{i,\mathcal{V}_i,s}^D}_{\text{desired signal}} + \underbrace{\sum_{k \in \mathcal{K}, k \neq i} z_{k,s} \mathbf{h}_{i,\mathcal{V}_k,s}^H \mathbf{x}_{k,\mathcal{V}_k,s}^D}_{\text{RAU-to-user interference}} + \underbrace{\sum_{j \in \mathcal{K}} z_{j,s} g_{i,j,s} x_{j,s}^U}_{\text{user-to-user interference}} + n_{i,s}^D, \quad (6)$$

subcarrier reuse interference

where $\mathbf{h}_{i,\mathcal{V}_i,s}^H \in \mathbb{C}^{1 \times V_i}$ represents the composite channel vector from virtual cell \mathcal{V}_i to user i on subcarrier s , $g_{i,j,s}$ denotes the composite channel from user j to user i on subcarrier s and $n_{i,s}^D \sim \mathcal{CN}(0, \sigma^2)$. In particular, $g_{i,i,s}$ denotes the residual self-interference coefficient from user i to itself, which is generated as $\mathbf{H}_{\text{SI},s}$.

The achievable spectral efficiency of user i in the downlink can be written as

$$R_i^D(\mathbf{P}, \mathbf{q}, \mathbf{z}) = \sum_{s \in \mathcal{S}} \log \left(1 + \frac{z_{i,s} \mathbf{h}_{i,\mathcal{V}_i,s}^H \mathbf{P}_{i,s} \mathbf{h}_{i,\mathcal{V}_i,s}}{\phi_{i,s}^D} \right). \quad (7)$$

where $\phi_{i,s}^D$ represents the interference-plus-noise of user i on subcarrier s in the downlink transmission, which is given by

$$\phi_{i,s}^D = \sum_{k \in \mathcal{K}, k \neq i} z_{k,s} \mathbf{h}_{i,\mathcal{V}_k,s}^H \mathbf{P}_{k,s} \mathbf{h}_{i,\mathcal{V}_k,s} + \sum_{j \in \mathcal{K}} z_{j,s} q_{j,s} |g_{i,j,s}|^2 + \sigma^2. \quad (8)$$

Then, the total system spectral efficiency is obtained as

$$R(\mathbf{P}, \mathbf{q}, \mathbf{z}) = \sum_{i \in \mathcal{K}} R_i^U(\mathbf{P}, \mathbf{q}, \mathbf{z}) + \sum_{i \in \mathcal{K}} R_i^D(\mathbf{P}, \mathbf{q}, \mathbf{z}). \quad (9)$$

B. Spectral Efficiency Problem Formulation

In this paper, our goal is to maximize the system spectral efficiency by jointly optimizing the downlink transmit power \mathbf{P} , the uplink transmit power \mathbf{q} , and subcarrier assignment \mathbf{z} under the per-user uplink/downlink transmit power constraints, subcarrier reuse, as well as the QoS requirement of each user both the uplink and downlink transmission. Specifically, the optimization problem can be formulated as

$$\max_{\mathbf{P}, \mathbf{q}, \mathbf{z}} R(\mathbf{P}, \mathbf{q}, \mathbf{z}) \quad (10a)$$

$$\text{s.t.} \quad \sum_{s \in \mathcal{S}} z_{i,s} q_{i,s} \leq q_{\max_i}, \forall i \in \mathcal{K}, \quad (10b)$$

$$q_{i,s} \geq 0, \forall i \in \mathcal{K}, s \in \mathcal{S}, \quad (10c)$$

$$\sum_{s \in \mathcal{S}} \text{Tr}(z_{i,s} \mathbf{P}_{i,s}) \leq p_{\max_i}, \forall i \in \mathcal{K}, \quad (10d)$$

$$p_{i,m,s} \geq 0, \forall i \in \mathcal{K}, m \in \mathcal{V}_i, s \in \mathcal{S}, \quad (10e)$$

$$R_i^U(\mathbf{P}, \mathbf{q}, \mathbf{z}) \geq R_{\min_i}^U, \forall i \in \mathcal{K}, \quad (10f)$$

$$R_i^D(\mathbf{P}, \mathbf{q}, \mathbf{z}) \geq R_{\min_i}^D, \forall i \in \mathcal{K}, \quad (10g)$$

$$\sum_{i \in \mathcal{K}} z_{i,s} \leq K_s, \forall s \in \mathcal{S}, \quad (10h)$$

$$z_{i,s} \in \{0, 1\}, \forall i \in \mathcal{K}, \forall s \in \mathcal{S}, \quad (10i)$$

where q_{\max_i} in (10b) is the maximum uplink transmit power of each user, and p_{\max_i} in (10d) is the maximum downlink

transmit power for each user. In (10f) and (10g), $R_{\min_i}^U$ and $R_{\min_i}^D$ denote the minimum data rate requirement for user i at the uplink and downlink, respectively. Constraint (10h) indicates that each subcarrier can be assigned to at most K_s users, which can avoid excessive interference. Constraint (10i) is a binary constraint for subcarrier assignment.

III. SPECTRAL EFFICIENCY MAXIMIZATION

Due to the non-convex objective function and constraints (10f) and (10g) as well as the binary constraint (10i), problem (10) is an MINLP optimization problem, which is NP-hard. Furthermore, discrete variable \mathbf{z} coupled with both downlink power variable \mathbf{P} and uplink power variable \mathbf{q} in objective function and constraints (10f) and (10g) make problem more intractable. The general method to solve this problem is to utilize hierarchical decomposition method, which decomposes the original problem into a subcarrier assignment subproblem and a power allocation subproblem and subsequently solves two subproblems separately. However, the effect of this method is usually not ideal. Exhaustive search is the optimal algorithm to solve the subcarrier assignment problem, in which $\left(\binom{K}{1} + \binom{K}{2} + \dots + \binom{K}{K_s}\right)^S$ possible subcarrier assignment sets will be searched, resulting it computationally prohibitive even for moderate values of K or S . In the following, we will develop an effective overall optimization algorithm to solve the optimization problem (10).

A. Spectral Efficiency Problem Reformulation

We first deal with the coupled binary variable \mathbf{z} and continuous variables \mathbf{P} and \mathbf{q} . Note that for the nonlinear cross multiplication terms $z_{i,s} q_{i,s}$ and $z_{i,s} \mathbf{P}_{i,s}$, if $z_{i,s} = 0$, $q_{i,s}$ and $\mathbf{P}_{i,s}$ are both equal to 0. To this end, we introduce two new auxiliary power variables $\tilde{\mathbf{P}}_{i,s} = z_{i,s} \mathbf{P}_{i,s}$ and $\tilde{q}_{i,s} = z_{i,s} q_{i,s}$ to replace the original optimized cross multiplication terms. Then, the original optimization variables \mathbf{P} and \mathbf{q} are replaced by auxiliary variables $\tilde{\mathbf{P}}$ and $\tilde{\mathbf{q}}$, respectively. Moreover, in order to be equivalent to constraints (10b) and (10d), we have added two power constraints as follows:

$$\tilde{q}_{i,s} \leq z_{i,s} q_{\max_i}, \forall i \in \mathcal{K}, s \in \mathcal{S} \quad (11)$$

and

$$\text{Tr}(\tilde{\mathbf{P}}_{i,s}) \leq z_{i,s} p_{\max_i}, \forall i \in \mathcal{K}, s \in \mathcal{S}. \quad (12)$$

Constraints (11) and (12) guarantee that $\tilde{q}_{i,s}$ and $\tilde{\mathbf{P}}_{i,s}$ are both equal to 0 if subcarrier s is not assigned to user i , i.e., when $z_{i,s} = 0$, $\tilde{q}_{i,s} = 0$ and $\tilde{\mathbf{P}}_{i,s} = 0$, respectively. Hence, we

rewrite the original optimization problem (10) as

$$\begin{aligned} \max_{\tilde{\mathbf{P}}, \tilde{\mathbf{q}}, \mathbf{z}} \quad & R(\tilde{\mathbf{P}}, \tilde{\mathbf{q}}) \quad (13a) \\ \text{s.t.} \quad & \sum_{s \in \mathcal{S}} \tilde{q}_{i,s} \leq q_{\max_i}, \forall i \in \mathcal{K}, \quad (13b) \\ & \tilde{q}_{i,s} \geq 0, \forall i \in \mathcal{K}, s \in \mathcal{S}, \quad (13c) \\ & \sum_{s \in \mathcal{S}} \text{Tr}(\tilde{\mathbf{P}}_{i,s}) \leq p_{\max_i}, \forall i \in \mathcal{K}, \quad (13d) \\ & \tilde{p}_{i,m,s} \geq 0, \forall i \in \mathcal{K}, m \in \mathcal{V}_i, s \in \mathcal{S}, \quad (13e) \\ & R_i^U(\tilde{\mathbf{P}}, \tilde{\mathbf{q}}) \geq R_{\min_i}^U, \forall i \in \mathcal{K}, \quad (13f) \\ & R_i^D(\tilde{\mathbf{P}}, \tilde{\mathbf{q}}) \geq R_{\min_i}^D, \forall i \in \mathcal{K}, \quad (13g) \\ & (10h), (10i), (11), (12). \quad (13h) \end{aligned}$$

Next, we rewrite the binary constraint (10i) to its equivalent form as

$$0 \leq z_{i,s} \leq 1, \forall i \in \mathcal{K}, s \in \mathcal{S} \quad (14)$$

and

$$\sum_{i \in \mathcal{K}} \sum_{s \in \mathcal{S}} (z_{i,s} - (z_{i,s})^2) \leq 0, \quad (15)$$

where (14) represents the binary variables $z_{i,s}$ are relaxed to continuous variables, (15) guarantees variables $z_{i,s}$ are binary values. Then, the problem (13) can be equivalently transformed as [21], [33]

$$\begin{aligned} \max_{\tilde{\mathbf{P}}, \tilde{\mathbf{q}}, \mathbf{z}} \quad & R(\tilde{\mathbf{P}}, \tilde{\mathbf{q}}) - \xi \sum_{i \in \mathcal{K}} \sum_{s \in \mathcal{S}} (z_{i,s} - (z_{i,s})^2) \quad (16a) \\ \text{s.t.} \quad & (13b) - (13g), (10h), (11), (12), (14), \quad (16b) \end{aligned}$$

where $\xi \gg 1$ is a large constant called penalty factor to penalize the objective function when $z_{i,s}$ is not equal to 0 or 1.

All the subsequent transformations are built upon an observation that the objective function of problem (16) and constraints (13f) and (13g) are the difference of two concave functions. Indeed, we can rewrite the function $R(\tilde{\mathbf{P}}, \tilde{\mathbf{q}}) = f_1(\tilde{\mathbf{P}}, \tilde{\mathbf{q}}) - f_2(\tilde{\mathbf{P}}, \tilde{\mathbf{q}})$, where

$$\begin{aligned} f_1(\tilde{\mathbf{P}}, \tilde{\mathbf{q}}) = & \sum_{i \in \mathcal{K}} \sum_{s \in \mathcal{S}} \log \left(\sum_{k \in \mathcal{K}} \mathbf{h}_{i,\mathcal{V}_k,s}^H \tilde{\mathbf{P}}_{k,s} \mathbf{h}_{i,\mathcal{V}_k,s} \right. \\ & \left. + \sum_{j \in \mathcal{K}} \tilde{q}_{j,s} |g_{i,j,s}|^2 + \sigma^2 \right) \\ & + \sum_{i \in \mathcal{K}} \sum_{s \in \mathcal{S}} \log \det \left(\sum_{k \in \mathcal{K}} \tilde{q}_{k,s} \mathbf{h}_{\mathcal{V}_i,k,s} \mathbf{h}_{\mathcal{V}_i,k,s}^H \right. \\ & \left. + \sum_{j \in \mathcal{K}} \mathbf{H}_{\text{SI},s} \tilde{\mathbf{P}}_{j,s} \mathbf{H}_{\text{SI},s}^H + \sigma^2 \mathbf{I}_{V_i} \right) \quad (17) \end{aligned}$$

and

$$\begin{aligned} f_2(\tilde{\mathbf{P}}, \tilde{\mathbf{q}}) = & \sum_{i \in \mathcal{K}} \sum_{s \in \mathcal{S}} \log \left(\sum_{k \in \mathcal{K}, k \neq i} \mathbf{h}_{i,\mathcal{V}_k,s}^H \tilde{\mathbf{P}}_{k,s} \mathbf{h}_{i,\mathcal{V}_k,s} \right. \\ & \left. + \sum_{j \in \mathcal{K}} \tilde{q}_{j,s} |g_{i,j,s}|^2 + \sigma^2 \right) \\ & + \sum_{i \in \mathcal{K}} \sum_{s \in \mathcal{S}} \log \det \left(\sum_{k \in \mathcal{K}, k \neq i} \tilde{q}_{k,s} \mathbf{h}_{\mathcal{V}_i,k,s} \mathbf{h}_{\mathcal{V}_i,k,s}^H \right. \\ & \left. + \sum_{j \in \mathcal{K}} \mathbf{H}_{\text{SI},s} \tilde{\mathbf{P}}_{j,s} \mathbf{H}_{\text{SI},s}^H + \sigma^2 \mathbf{I}_{V_i} \right). \quad (18) \end{aligned}$$

The objective function of problem (16) can be expressed as

$$g_1(\tilde{\mathbf{P}}, \tilde{\mathbf{q}}, \mathbf{z}) - g_2(\tilde{\mathbf{P}}, \tilde{\mathbf{q}}, \mathbf{z}), \quad (19)$$

where

$$g_1(\tilde{\mathbf{P}}, \tilde{\mathbf{q}}, \mathbf{z}) = f_1(\tilde{\mathbf{P}}, \tilde{\mathbf{q}}) - \xi \sum_{i \in \mathcal{K}} \sum_{s \in \mathcal{S}} z_{i,s} \quad (20)$$

and

$$g_2(\tilde{\mathbf{P}}, \tilde{\mathbf{q}}, \mathbf{z}) = f_2(\tilde{\mathbf{P}}, \tilde{\mathbf{q}}) - \xi \sum_{i \in \mathcal{K}} \sum_{s \in \mathcal{S}} (z_{i,s})^2. \quad (21)$$

One can see that both functions $g_1(\tilde{\mathbf{P}}, \tilde{\mathbf{q}}, \mathbf{z})$ and $g_2(\tilde{\mathbf{P}}, \tilde{\mathbf{q}}, \mathbf{z})$ are jointly concave in $(\tilde{\mathbf{P}}, \tilde{\mathbf{q}}, \mathbf{z})$, i.e., the objective function of problem (16) is the difference of two convex functions structure. We define the value of $(\tilde{\mathbf{P}}, \tilde{\mathbf{q}}, \mathbf{z})$ at d -th iteration is $(\tilde{\mathbf{P}}^{(d)}, \tilde{\mathbf{q}}^{(d)}, \mathbf{z}^{(d)})$, and then we can find an linear function to replace $g_2(\tilde{\mathbf{P}}, \tilde{\mathbf{q}}, \mathbf{z})$ by using the first-order Taylor approximation as

$$\begin{aligned} g_2^{(d)}(\tilde{\mathbf{P}}, \tilde{\mathbf{q}}, \mathbf{z}) = & f_2(\tilde{\mathbf{P}}^{(d)}, \tilde{\mathbf{q}}^{(d)}) - \xi \sum_{i \in \mathcal{K}} \sum_{s \in \mathcal{S}} (z_{i,s}^{(d)})^2 \\ & + \sum_{i \in \mathcal{K}} \sum_{s \in \mathcal{S}} \sum_{k \in \mathcal{K}, k \neq i} \left(\vartheta^{(d)} \right)^{-1} \mathbf{h}_{i,\mathcal{V}_k,s}^H \left(\tilde{\mathbf{P}}_{k,s} - \tilde{\mathbf{P}}_{k,s}^{(d)} \right) \mathbf{h}_{i,\mathcal{V}_k,s} \\ & + \sum_{i \in \mathcal{K}} \sum_{s \in \mathcal{S}} \sum_{j \in \mathcal{K}} \left(\vartheta^{(d)} \right)^{-1} |g_{i,j,s}|^2 \left(\tilde{q}_{j,s} - \tilde{q}_{j,s}^{(d)} \right) \\ & + \sum_{i \in \mathcal{K}} \sum_{s \in \mathcal{S}} \sum_{k \in \mathcal{K}, k \neq i} \text{Tr} \left[\left(\psi^{(d)} \right)^{-1} \mathbf{h}_{\mathcal{V}_i,k,s} \mathbf{h}_{\mathcal{V}_i,k,s}^H \left(\tilde{q}_{k,s} - \tilde{q}_{k,s}^{(d)} \right) \right] \\ & + \sum_{i \in \mathcal{K}} \sum_{s \in \mathcal{S}} \sum_{j \in \mathcal{K}} \text{Tr} \left[\mathbf{H}_{\text{SI},s} \left(\psi^{(d)} \right)^{-1} \mathbf{H}_{\text{SI},s} \left(\tilde{\mathbf{P}}_{j,s} - \tilde{\mathbf{P}}_{j,s}^{(d)} \right) \right] \\ & - \xi \sum_{i \in \mathcal{K}} \sum_{s \in \mathcal{S}} 2 \left(z_{i,s}^{(d)} \right) \left(z_{i,s} - z_{i,s}^{(d)} \right), \quad (22) \end{aligned}$$

where

$$\vartheta^{(d)} = \sum_{k \in \mathcal{K}, k \neq i} \mathbf{h}_{i,\mathcal{V}_k,s}^H \tilde{\mathbf{P}}_{k,s}^{(d)} \mathbf{h}_{i,\mathcal{V}_k,s} + \sum_{j \in \mathcal{K}} \tilde{p}_{j,s}^{(d)} |g_{i,j,s}|^2 + \sigma^2 \quad (23)$$

and

$$\psi^{(d)} = \sum_{k \in \mathcal{K}, k \neq i} \tilde{q}_{k,s}^{(d)} \mathbf{h}_{\mathcal{V}_i,k,s} \mathbf{h}_{\mathcal{V}_i,k,s}^H + \sum_{j \in \mathcal{K}} \mathbf{H}_{\text{SI},s} \tilde{\mathbf{P}}_{j,s}^{(d)} \mathbf{H}_{\text{SI},s}^H + \sigma^2 \mathbf{I}_{V_i}. \quad (24)$$

After the linearization, the objective function of problem (16) is transformed to a concave function.

Following similar processes, we can approximate the constraints (13f) and (13g) by convex constraint. The uplink QoS constraint (13f) can be approximated as

$$f_i^U(\tilde{\mathbf{P}}, \tilde{\mathbf{q}}) - g_i^U(\tilde{\mathbf{P}}, \tilde{\mathbf{q}}) \geq R_{\min,i}^U, \forall i \in \mathcal{K}, \quad (25)$$

where

$$f_i^U(\tilde{\mathbf{P}}, \tilde{\mathbf{q}}) = \sum_{s \in \mathcal{S}} \log \det \left(\sum_{k \in \mathcal{K}} \tilde{q}_{k,s} \mathbf{h}_{\mathcal{V}_i,k,s} \mathbf{h}_{\mathcal{V}_i,k,s}^H + \sum_{j \in \mathcal{K}} \mathbf{H}_{\text{SI},s} \tilde{\mathbf{P}}_{j,s} \mathbf{H}_{\text{SI},s}^H + \sigma^2 \mathbf{I}_{V_i} \right) \quad (26)$$

and

$$g_i^U(\tilde{\mathbf{P}}, \tilde{\mathbf{q}}) = g_i^U(\tilde{\mathbf{P}}^{(d)}, \tilde{\mathbf{q}}^{(d)}) + \sum_{s \in \mathcal{S}} \sum_{k \in \mathcal{K}, k \neq i} \text{Tr} \left[\left(\psi^{(d)} \right)^{-1} \mathbf{h}_{\mathcal{V}_i,k,s} \mathbf{h}_{\mathcal{V}_i,k,s}^H \left(\tilde{q}_{k,s} - \tilde{q}_{k,s}^{(d)} \right) \right] + \sum_{s \in \mathcal{S}} \sum_{j \in \mathcal{K}} \text{Tr} \left[\mathbf{H}_{\text{SI},s}^H \left(\psi^{(d)} \right)^{-1} \mathbf{H}_{\text{SI},s} \left(\tilde{\mathbf{P}}_{j,s} - \tilde{\mathbf{P}}_{j,s}^{(d)} \right) \right]. \quad (27)$$

The downlink QoS constraint (13g) can be approximated as

$$f_i^D(\tilde{\mathbf{P}}, \tilde{\mathbf{q}}) - g_i^D(\tilde{\mathbf{P}}, \tilde{\mathbf{q}}) \geq R_{\min,i}^D, \forall i \in \mathcal{K} \quad (28)$$

where

$$f_i^D(\tilde{\mathbf{P}}, \tilde{\mathbf{q}}) = \sum_{s \in \mathcal{S}} \log \left(\sum_{k \in \mathcal{K}} \mathbf{h}_{i,\mathcal{V}_k,s}^H \tilde{\mathbf{P}}_{k,s} \mathbf{h}_{i,\mathcal{V}_k,s} + \sum_{j \in \mathcal{K}} \tilde{q}_{j,s} |g_{i,j,s}|^2 + \sigma^2 \right) \quad (29)$$

and

$$g_i^D(\tilde{\mathbf{P}}, \tilde{\mathbf{q}}) = g_i^D(\tilde{\mathbf{P}}^{(d)}, \tilde{\mathbf{q}}^{(d)}) + \sum_{s \in \mathcal{S}} \sum_{k \in \mathcal{K}, k \neq i} \left(\vartheta^{(d)} \right)^{-1} \mathbf{h}_{i,\mathcal{V}_k,s}^H \left(\tilde{\mathbf{P}}_{k,s} - \tilde{\mathbf{P}}_{k,s}^{(d)} \right) \mathbf{h}_{i,\mathcal{V}_k,s} + \sum_{s \in \mathcal{S}} \sum_{j \in \mathcal{K}} \left(\vartheta^{(d)} \right)^{-1} |g_{i,j,s}|^2 \left(\tilde{q}_{j,s} - \tilde{q}_{j,s}^{(d)} \right). \quad (30)$$

Hence, we can reformulate the problem (16) as the following problem:

$$\max_{\tilde{\mathbf{P}}, \tilde{\mathbf{q}}, \mathbf{z}} g_1(\tilde{\mathbf{P}}, \tilde{\mathbf{q}}, \mathbf{z}) - g_2^{(d)}(\tilde{\mathbf{P}}, \tilde{\mathbf{q}}, \mathbf{z}) \quad (31a)$$

$$\text{s.t.} \quad (13b) - (13e), (10h), (11), (12), (14), (25), (28). \quad (31b)$$

The optimization problem (31) is a convex problem, which can be solved by interior-point methods or specific convex software packages such as CVX [35] and MOSEK [36]. The

iterative algorithm for solving the problem (31) is summarized in Algorithm 1 and the monotonic convergence to the locally optimal solution is guaranteed.

Proof: Please refer to Appendix A for the proof of convergence. ■

Algorithm 1 : Algorithm for Solving Problem (31)

- 1: Initialization: Each user $i \in \mathcal{K}$ selects V_i RAUs with the largest large-scale fading to form its virtual cell. Generate the initial values for $\{\tilde{\mathbf{P}}, \tilde{\mathbf{q}}, \mathbf{z}\}^{(0)}$, penalty factor $\xi \gg 1$, maximum tolerance $\omega = 10^{-3}$.
- 2: Set $d = 0$.
- 3: **Repeat**
- 4: Solve (31) with $\{\mathbf{p}, \mathbf{q}, \mathbf{z}\}^{(0)}$ to obtain the optimal solutions $\{\tilde{\mathbf{P}}^*, \tilde{\mathbf{q}}^*, \mathbf{z}^*\}$.
- 5: Update $\{\tilde{\mathbf{P}}^{(d+1)}, \tilde{\mathbf{q}}^{(d+1)}, \mathbf{z}^{(d+1)}\} = \{\tilde{\mathbf{P}}^*, \tilde{\mathbf{q}}^*, \mathbf{z}^*\}$.
- 6: Set $d = d + 1$.
- 7: **Until** convergence.
- 8: Return $\tilde{\mathbf{P}}^*, \tilde{\mathbf{q}}^*$ and \mathbf{z}^* .

B. Computational Complexity and Signaling Overhead Analysis

In the OFDMA-based FD DAS considered in this work, the proposed joint subcarrier assignment and power allocation algorithm is performed at the BBU. Specifically, the BBU is required to collect the large-scale fading between each user and all RAUs to form each user's virtual cell. Therefore, only the instantaneous CSI between each user and all user's virtual cells, as well as between all users is required for the subsequent steps of Algorithm 1, and thus the number of channels that need to be measured becomes small. The amount of CSI signaling overhead is limited by the pilot training frequency and the amount of information in each report, in which the training frequency depends on the user movement speed³.

Due to the application of the user-centric strategy, each user can only be served by its virtual cell, the optimization problem (31) contains $2KS + \sum_{i \in \mathcal{K}} SV_i$ variables and $4KS + 4K + S + \sum_{i \in \mathcal{K}} SV_i$ convex constraints, whose computational complexity is $\mathcal{O}\left((2KS + \sum_{i \in \mathcal{K}} SV_i)^3 (4KS + 4K + S + \sum_{i \in \mathcal{K}} SV_i)\right)$ and can be guaranteed in polynomial time [37], [38]. In contrast, if all RAUs serve each user, there are $2KS + KNS$ decision variables, which will cause high computational complexity in the presence of a large number of RAUs, users and subcarriers.

IV. SIMULATION RESULTS

A. Simulation Setup

In this section, we present simulation results to evaluate the performance of our proposed algorithm. We consider a square

³A quasi-static channel model is considered in this work, in which we assume the channel is essentially constant over a short period. The high user mobility will be considered in our future work.

coverage area, where N RAUs and K users are uniformly distributed in each independent experiment. The experiment parameters are set based on existing 3rd generation partnership project (3GPP) specifications [39]–[41]. We set the subcarrier bandwidth as 180 kHz. The standard deviation of shadowing is set to be 8 dB. The noise power is -107 dBm, and the path loss exponent is set to be 4. The penalty factor ξ is set to be 10^4 . For simplicity, we assume the same virtual cell size for all users, i.e., $|\mathcal{V}_i| = V, \forall i \in \mathcal{K}$. All users have the identical power constraints $p_{\max_i} = p_{\max}$ and $q_{\max_i} = q_{\max}, \forall i \in \mathcal{K}$, and all users require identical minimum rate, i.e. $R_{\min_i}^U = R_{\min_i}^D = R_{\min}, \forall i \in \mathcal{K}$. Unless specified otherwise, we assume cell length $D_0 = 1000$ m, $p_{\max} = 30$ dBm, $q_{\max} = 21$ dBm, $V = 3$, $a = 1$, $R_{\min} = 1$ bits/s/Hz and $\sigma_{\text{SI}}^2 = -100$ dB. We compare our proposed algorithm with existing schemes proposed in [17], [28], and the following algorithms:

- **Exhaustive search:** This algorithm first lists all possible subcarrier assignment sets, then uses our proposed algorithm to perform the power allocation for each possible set, and finally finds the maximum value as the solution of the problem. The computational complexity of this scheme is $\mathcal{O}\left(\left(\binom{K}{1} + \binom{K}{2} + \dots + \binom{K}{K_s}\right)^S \times (KS + \sum_{i \in \mathcal{K}} SV_i)^3 (KS + 4K + \sum_{i \in \mathcal{K}} SV_i)\right)$.
- **Hierarchical decomposition:** This algorithm decomposes the original optimization problem into two subproblems of subcarrier assignment and power allocation. Get the optimal subcarrier assignment set through exhaustive exhaustion, and then use our proposed algorithm to find the solution of power allocation subproblem. The computational complexity of this scheme is $\mathcal{O}\left(\left(\binom{K}{1} + \binom{K}{2} + \dots + \binom{K}{K_s}\right)^S + (KS + \sum_{i \in \mathcal{K}} SV_i)^3 (KS + 4K + \sum_{i \in \mathcal{K}} SV_i)\right)$.
- **Exclusive subcarrier assignment:** This scheme corresponds to the case that sets $K_s = 1$ in our proposed algorithm, that is, each subcarrier can be assigned to at most one user. The computational complexity of this scheme is the same as our proposed algorithm.
- **HD scheme:** The proposed algorithm is applied to HD operation. For the sake of fair comparison between HD and FD systems, time is assumed to be divided into two equal non-overlapping parts for downlink and uplink respectively, other system parameters are the same as the FD scheme. The complexity of the uplink transmission and downlink transmission is $\mathcal{O}\left((2KS)^3 (3KS + 2K + S)\right)$ and $\mathcal{O}\left((KS + \sum_{i \in \mathcal{K}} SV_i)^3 (2KS + 2K + S + \sum_{i \in \mathcal{K}} SV_i)\right)$, respectively.

B. Convergence speed of the Proposed Algorithm

Fig. 2 illustrates the convergence speed of the proposed algorithm for different configurations with the number of RAUs $N = 16$ and $K_s = 2$. We can observe that the spectral efficiency monotonically increases during the iteration process

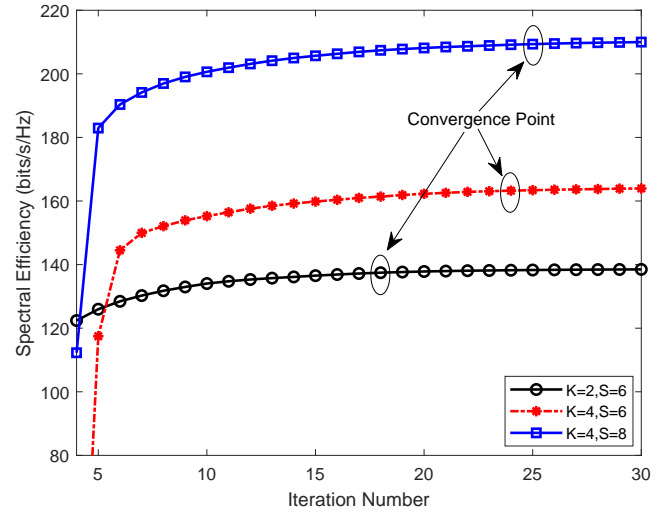


Fig. 2. Spectral efficiency versus the number of iterations for different K and S .

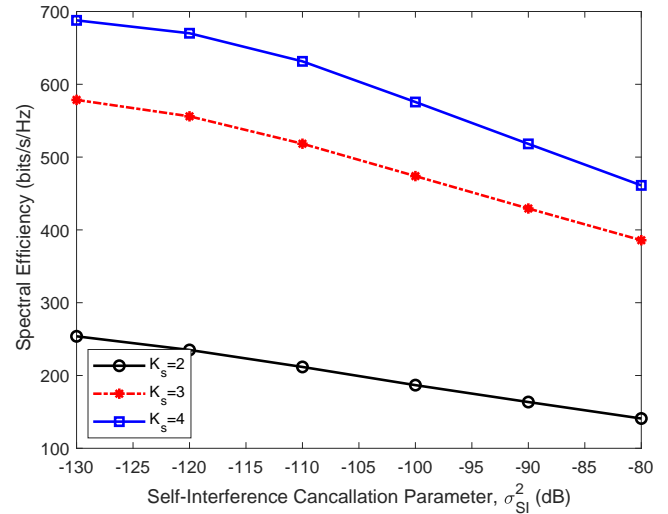


Fig. 3. Spectral efficiency versus σ_{SI}^2 (dB) with different K_s .

and converges within 30 iterations for all cases. Also, we can see that a larger K or S has higher spectral efficiency but needs more iterations to converge.

C. Effect of Self-interference Cancellation on the Performance of Different K_s

Fig. 3 shows the spectral efficiency versus the self-interference cancellation parameter σ_{SI}^2 for different K_s , where the number of users $K = 6$, the number of RAUs $N = 36$, and the number of subcarriers $S = 12$. We can observe from Fig. 3 that the spectral efficiency of all cases decreases as the residual self-interference cancellation parameter σ_{SI}^2 increases. This result shows that the ability to eliminate self-interference is the key to determining the performance of the FD system. From Fig. 3, we also see that the spectral efficiency is affected by K_s ; the larger K_s corresponds to the higher spectral efficiency.

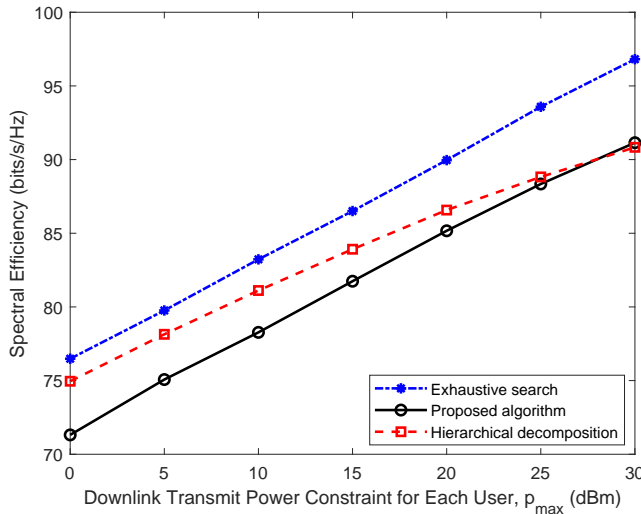


Fig. 4. Spectral efficiency versus the downlink maximum transmit power for each user.

D. Effect of Maximum Transmit Power on the Performance of Different Algorithms

Fig. 4 demonstrates the spectral efficiency versus the transmit power constraint for the proposed algorithm, the exhaustive search algorithm, and the hierarchical decomposition method using the optimal subcarrier allocation scheme. In this experiment, we set the number of users $K = 3$, the number of RAUs $N = 10$, the number of subcarriers $S = 6$, $K_s = 2$, $D_0 = 500$ m and $q_{\max} = 0.7p_{\max}$. We can see that the spectral efficiency increases with increasing the transmit power constraint for all cases. From Fig. 4, we can also observe that the proposed algorithm performs close to the exhaustive search algorithm, and their performance gap is about 7%, but the complexity of our proposed algorithm is much lower. In the relatively low transmit power constraint region, the performance of the proposed algorithm is slightly worse than the hierarchical decomposition method. This is because when the transmit power constraint is small, the interference is small, the subcarriers are more likely to be assigned to users based on channel gain; therefore, the hierarchical decomposition method benefits from exhaustive search. Also, note that the proposed algorithm can achieve almost 95% of the performance of the hierarchical decomposition method in the worst case when $p_{\max} = 0$ but has much lower complexity than the latter. As the transmit power constraint increases, the interference increases, the superiority of the overall optimization gradually becomes noticeable. When the transmit power constraint is large enough, the proposed algorithm outperforms the hierarchical decomposition method.

The running time of the above three algorithms is listed in Table I. We can see that the running time of the exhaustive search algorithm is much more than the proposed algorithm. It can also be observed that the running time of the proposed algorithm and the hierarchical decomposition method increases with the increase of K and S , but the time-consuming growth rate of the hierarchical decomposition method is much greater

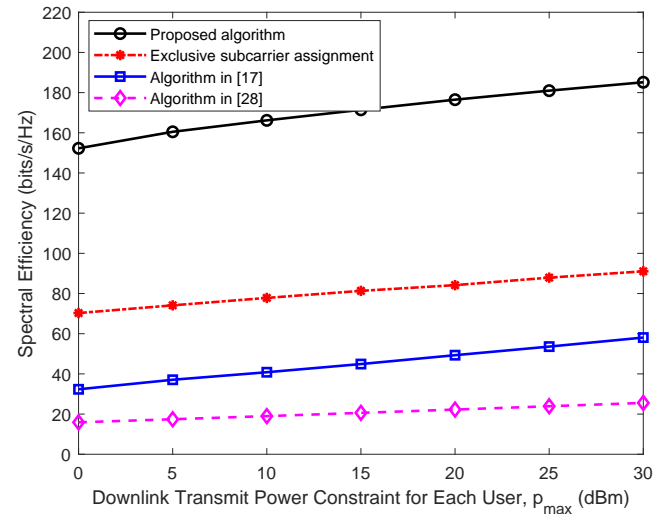


Fig. 5. Spectral efficiency versus the downlink maximum transmit power for each user.

than that of the proposed algorithm, which is consistent with the comparison of their complexity.

TABLE I
RUNNING TIME COMPARISON

Algorithm	Running time (s)		
	(K, S)		
	(3,3)	(3,8)	(4,8)
Exhaustive search	7897.853	-	-
Hierarchical decomposition	83.48	13907.975	-
Proposed algorithm	98.52	164.58	326.13

In Fig. 5, we compare the performance of the proposed algorithm with other related algorithms, including the exclusive subcarrier assignment algorithm and the algorithms proposed in [17] and [28]. Here, we set the number of users $K = 5$, the number of RAUs $N = 10$, the number of subcarriers $S = 5$, $D_0 = 500$ m, $K_s = 3$, and $q_{\max} = 0.7p_{\max}$. For a fair comparison, we assume that all scenarios have the same total downlink maximum transmit power and the same per-user uplink transmit power constraint. Since the studies in [17] and [28] do not consider the users' minimum rate requirements, we set $R_{\min} = 0$ in this experiment. We observe that our proposed algorithm outperforms all benchmark algorithms. This is because the performance gain over the algorithm proposed in [17] is due to the fact that [17] considers a single-antenna system, while we consider DAS, which can benefit from the multi-antenna diversity gain. On the other hand, the algorithm proposed in [28] just considers HD operation, while our algorithm considers FD transmission. Besides, the algorithms proposed in [17] and [28] are both heuristic algorithms, which decompose the problem into several subproblems to solve, while our proposed algorithm performs overall optimization and achieves near-exhaustive search performance. Moreover, the proposed algorithm allows subcarrier reuse to improve system performance compared with the exclusive subcarrier

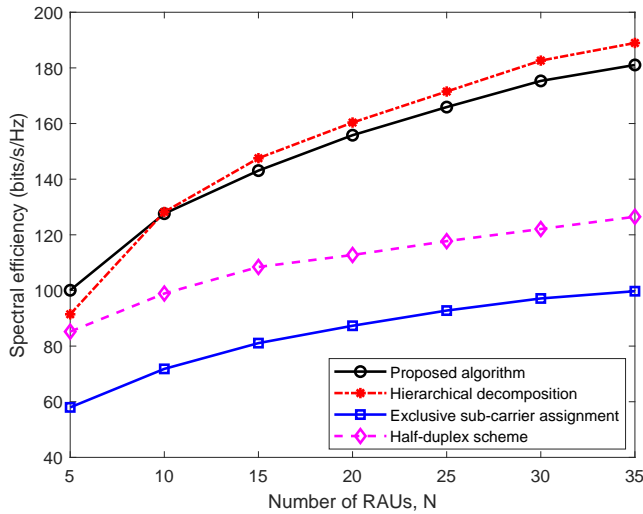


Fig. 6. Spectral efficiency versus the number of RAUs for different algorithms.

assignment scheme.

E. Effect of Number of RAUs on the Performance of Different Algorithms

Fig. 6 shows the spectral efficiency versus the number of RAUs for different algorithms. In this experiment, we set the number of users $K = 3$, the number of subcarriers $S = 6$, and $K_s = 2$. We can observe that the spectral efficiency of all algorithms improves with an increase in the number of RAUs. This is because that as the number of RAUs increases, the average access distance decreases, resulting in increased spectral efficiency. We also see that when the number of RAUs increases, the marginal increment of the spectral efficiency becomes smaller, indicating that further increasing the number of RAUs is negligible for spectral efficiency improvement. From Fig. 6, we can also see that the proposed algorithm outperforms the exclusive subcarrier assignment and HD schemes. In particular, when $N = 35$, the spectral efficiency of the proposed algorithm is approximately 81.54% and 43.14% higher than the exclusive subcarrier assignment scheme and the HD scheme, respectively. In the relatively small N region, the proposed algorithm outperforms the hierarchical decomposition method. The reason is when the number of RAUs is relatively small, different users' virtual cells would overlap or even be completely identical, which means there is strong interference between users. Therefore, more coordination gain can be obtained by the proposed algorithm from the overall optimization. As the increasing of the total number of RAUs, the virtual cell of each user is getting closer to the user, and the overlap of different virtual cells is gradually reduced, which indicates that the virtual cell of each user is gradually moving away from other users on average; therefore the effect of interference gradually diminishes, the hierarchical decomposition method obtains the higher performance benefitting from exhaustive search. In addition, the exclusive subcarrier assignment scheme is the

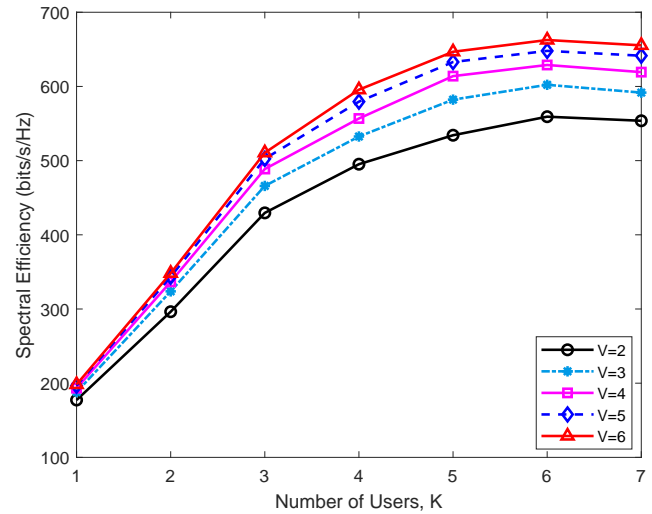


Fig. 7. Spectral efficiency versus the number of users with different V .

worst one, which implies that subcarrier reuse is quite effective for improving spectral efficiency.

F. Effect of Number of Users on the Performance of Different Virtual Cell Sizes

Fig. 7 illustrates the spectral efficiency versus the number of users K for different virtual cell size V . In this experiment, we set the number of RAUs $N = 36$, the number of subcarriers $S = 12$, and $K_s = 4$. We can see from Fig. 7 that for all V , as the number of users increases, the spectral efficiency will first increase and then decrease. The reason behind this observation can be explained as follows. The increase of K will cause more interference. Just for this reason, the performance improvement contributed by the newly added user gradually decreases. Meanwhile, the system is required to meet the QoS requirements of each user. Therefore, when the increase of K exceeds a threshold, the spectral efficiency begins to decline. From Fig. 7, we also observe that the spectral efficiency is higher with a larger V for all K , and the performance gap becomes larger as K increases. This implies that as the number of K increases, more RAUs should be included in each user's virtual cell to improve spectral efficiency. However, it should be noted that the newly added RAU in each user's virtual cell gradually moves away from the user, and thus its contribution gradually decreases. Besides, the larger the virtual cell size V , the higher the corresponding computational and signaling overhead. Therefore, the virtual cell size should be chosen carefully according to the practical scenarios.

G. Effect of Users' Minimum Rate Requirements on the Performance of Different Cell Lengths

Fig. 8 demonstrates the spectral efficiency versus users' minimum rate requirements for different cell lengths. In this experiment, we set the number of RAUs $N = 36$, the number of users $K = 6$, the number of subcarriers $S = 12$,

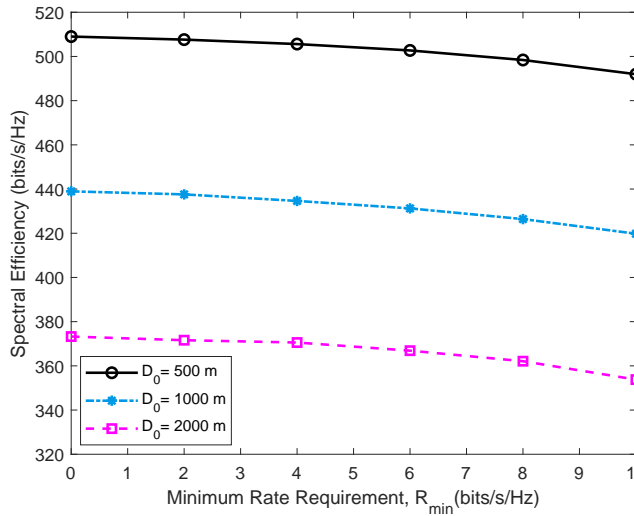


Fig. 8. Spectral efficiency versus users' minimum rate requirements with different cell lengths.

and $K_s = 3$. From Fig. 8, We observe that the spectral efficiency decreases with increasing the users' minimum rate requirements. This is because as the users' minimum rate requirements increase, the system will allocate more resources to users with poor performance subsequently lower spectral efficiency. But we also observe that the decline in the spectral efficiency is not significant, indicating that our proposed algorithm has a small cost of system performance while ensuring fairness among users. Besides, Fig. 8 also shows that the spectral efficiency increases as the cell length decreases. The reason is that as the cell length decreases, the reduced access distance results in increased spectral efficiency.

V. CONCLUSIONS

In this paper, the resource allocation in OFDMA-based FD DASs with users' uplink/downlink QoS requirements and subcarrier reuse was investigated. We jointly optimized the uplink/downlink transmit power and subcarrier assignment to maximize the system spectral efficiency. The user-centric virtual cell approach was adopted to reduce the computational and signaling overhead. We proposed an efficient overall optimization algorithm based on the successive convex approximation method and penalty factor to solve the formulated non-convex problem. In addition, we proved the convergence of the proposed algorithm and analyzed the computational and signaling overhead of the algorithm. Simulation results demonstrated that compared with the hierarchical decomposition algorithm adopting the optimal subcarrier allocation scheme, our proposed algorithm with lower complexity achieves higher performance in the interference-limited scenarios while obtaining comparable results with little interference. Besides, results showed that, the proposed algorithm can achieve a performance close to the exhaustive search algorithm and perform much better than other benchmark schemes. Furthermore, our proposed algorithm had little impact on system performance while ensuring user fairness.

The high user mobility is an interesting extension of our work. In this case, the dynamic network environment involving user mobile modeling and switching of virtual cells makes the optimization of resource allocation more complicated and challenging.

APPENDIX A

PROOF OF ALGORITHM CONVERGENCE

Since function $g_2(\tilde{\mathbf{P}}, \tilde{\mathbf{q}}, \mathbf{z})$ is concave,

$$g_2(\tilde{\mathbf{P}}, \tilde{\mathbf{q}}, \mathbf{z}) \leq g_2^{(d)}(\tilde{\mathbf{P}}, \tilde{\mathbf{q}}, \mathbf{z}). \quad (32)$$

Also we note that when $(\tilde{\mathbf{P}}, \tilde{\mathbf{q}}, \mathbf{z}) = (\tilde{\mathbf{P}}^{(d)}, \tilde{\mathbf{q}}^{(d)}, \mathbf{z}^{(d)})$,

$$g_2^{(d)}(\tilde{\mathbf{P}}^{(d)}, \tilde{\mathbf{q}}^{(d)}, \mathbf{z}^{(d)}) = f_2(\tilde{\mathbf{P}}^{(d)}, \tilde{\mathbf{q}}^{(d)}) - \xi \sum_{i \in \mathcal{K}} \sum_{s \in \mathcal{S}} (z_{i,s}^{(d)})^2. \quad (33)$$

Therefore, the objective function of problem (31) is a tight lower bound of the original problem, and

$$\begin{aligned} & g_1(\tilde{\mathbf{P}}^{(d+1)}, \tilde{\mathbf{q}}^{(d+1)}, \mathbf{z}^{(d+1)}) - g_2(\tilde{\mathbf{P}}^{(d+1)}, \tilde{\mathbf{q}}^{(d+1)}, \mathbf{z}^{(d+1)}) \\ & \geq g_1(\tilde{\mathbf{P}}^{(d+1)}, \tilde{\mathbf{q}}^{(d+1)}, \mathbf{z}^{(d+1)}) - g_2^{(d)}(\tilde{\mathbf{P}}^{(d+1)}, \tilde{\mathbf{q}}^{(d+1)}, \mathbf{z}^{(d+1)}) \\ & = \max_{\tilde{\mathbf{P}}, \tilde{\mathbf{q}}, \mathbf{z}} g_1(\tilde{\mathbf{P}}, \tilde{\mathbf{q}}, \mathbf{z}) - g_2^{(d)}(\tilde{\mathbf{P}}, \tilde{\mathbf{q}}, \mathbf{z}) \\ & \geq g_1(\tilde{\mathbf{P}}^{(d)}, \tilde{\mathbf{q}}^{(d)}, \mathbf{z}^{(d)}) - g_2^{(d)}(\tilde{\mathbf{P}}^{(d)}, \tilde{\mathbf{q}}^{(d)}, \mathbf{z}^{(d)}) \\ & = g_1(\tilde{\mathbf{P}}^{(d)}, \tilde{\mathbf{q}}^{(d)}, \mathbf{z}^{(d)}) - g_2(\tilde{\mathbf{P}}^{(d)}, \tilde{\mathbf{q}}^{(d)}, \mathbf{z}^{(d)}) \end{aligned} \quad (34)$$

which means that the optimal solution obtained in the $(d+1)$ -th iteration is greater than the optimal solution obtained in the d -th iteration. Due to the constraints are compact, the proposed algorithm guarantees monotonic convergence to the locally optimal solution.

REFERENCES

- [1] C. Wang, J. Huang, H. Wang, X. Gao, X. You, and Y. Hao, "6G wireless channel measurements and models: Trends and challenges," *IEEE Veh. Technol. Mag.*, vol. 15, no. 4, pp. 22–32, 2020.
- [2] C. Liang and F. R. Yu, "Wireless network virtualization: A survey, some research issues and challenges," *IEEE Commun. Surv. Tutor.*, vol. 17, no. 1, pp. 358–380, 2015.
- [3] T. Alade, H. Zhu, and J. Wang, "Uplink spectral efficiency analysis of in-building distributed antenna systems," *IEEE Trans. Wireless Commun.*, vol. 14, no. 7, pp. 4063–4074, 2015.
- [4] Y. Zhang and L. Dai, "A closed-form approximation for uplink average ergodic sum capacity of large-scale multi-user distributed antenna systems," *IEEE Trans. Veh. Technol.*, vol. 68, no. 2, pp. 1745–1756, 2019.
- [5] J. Li, D. Wang, P. Zhu, J. Wang, and X. You, "Downlink spectral efficiency of distributed massive MIMO systems with linear beamforming under pilot contamination," *IEEE Trans. Veh. Technol.*, vol. 67, no. 2, pp. 1130–1145, 2018.
- [6] J. Wang and L. Dai, "Downlink rate analysis for virtual-cell based large-scale distributed antenna systems," *IEEE Trans. Wireless Commun.*, vol. 15, no. 3, pp. 1998–2011, 2016.
- [7] Z. Zhang, X. Chai, K. Long, A. V. Vasilakos, and L. Hanzo, "Full duplex techniques for 5G networks: self-interference cancellation, protocol design, and relay selection," *IEEE Commun. Mag.*, vol. 53, no. 5, pp. 128–137, 2015.
- [8] M. Duarte, C. Dick, and A. Sabharwal, "Experiment-driven characterization of full-duplex wireless systems," *IEEE Trans. Wireless Commun.*, vol. 11, no. 12, pp. 4296–4307, 2012.

- [9] D. Bharadia, E. Mcmilin, and S. Katti, "Full duplex radios," *Comput. Commun. Review*, vol. 43, no. 4, pp. 375–386, 2013.
- [10] A. Masmoudi and T. Le-Ngoc, "Self-interference cancellation limits in full-duplex communication systems," in *Proc. IEEE Global Commun. Conf.*, Washington, Dec. 2016, pp. 1–6.
- [11] A. Jindal and Z. J. Haas, "On the performance of distributed MIMO with full-duplex jamming," *IEEE Trans. Commun.*, vol. 67, no. 3, pp. 1972–1985, 2019.
- [12] Y. Li, P. Fan, A. Leukhin, and L. Liu, "On the spectral and energy efficiency of full-duplex small-cell wireless systems with massive MIMO," *IEEE Trans. Veh. Technol.*, vol. 66, no. 3, pp. 2339–2353, 2017.
- [13] O. Simeone, E. Erkip, and S. Shamaï, "Full-duplex cloud radio access networks: An information-theoretic viewpoint," *IEEE Wireless Commun. Lett.*, vol. 3, no. 4, pp. 413–416, 2014.
- [14] W. Tang and S. Feng, "User selection and power minimization in full-duplex cloud radio access networks," *IEEE Trans. Signal Process.*, vol. 67, no. 9, pp. 2426–2438, 2019.
- [15] A. Shojaefard, K. Wong, W. Yu, G. Zheng, and J. Tang, "Full-duplex cloud radio access network: Stochastic design and analysis," *IEEE Trans. Wireless Commun.*, vol. 17, no. 11, pp. 7190–7207, 2018.
- [16] M. Mohammadi, H. A. Suraweera, and C. Tellambura, "Uplink/downlink rate analysis and impact of power allocation for full-duplex cloud-RANs," *IEEE Trans. Wireless Commun.*, vol. 17, no. 9, pp. 5774–5788, 2018.
- [17] B. Di, S. Bayat, L. Song, Y. Li, and Z. Han, "Joint user pairing, subchannel, and power allocation in full-duplex multi-user OFDMA networks," *IEEE Trans. Wireless Commun.*, vol. 15, no. 12, pp. 8260–8272, 2016.
- [18] R. Sultan, L. Song, K. G. Seddik, and Z. Han, "Joint resource management with distributed uplink power control in full-duplex OFDMA networks," *IEEE Trans. Veh. Technol.*, vol. 69, no. 3, pp. 2850–2863, 2020.
- [19] C. Nam, C. Joo, and S. Bahk, "Joint subcarrier assignment and power allocation in full-duplex OFDMA networks," *IEEE Trans. Wireless Commun.*, vol. 14, no. 6, pp. 3108–3119, 2015.
- [20] H. Kim, H. Lee, M. Ahn, H. Kong, and I. Lee, "Joint subcarrier and power allocation methods in full duplex wireless powered communication networks for OFDM systems," *IEEE Trans. Wireless Commun.*, vol. 15, no. 7, pp. 4745–4753, 2016.
- [21] R. Aslani, M. Rasti, and A. Khalili, "Energy efficiency maximization via joint sub-carrier assignment and power control for OFDMA full duplex networks," *IEEE Trans. Veh. Technol.*, vol. 68, no. 12, pp. 11 859–11 872, 2019.
- [22] S. Zarandi, A. Khalili, M. Rasti, and H. Tabassum, "Multi-objective energy efficient resource allocation and user association for in-band full duplex small-cells," *IEEE Trans. Green Commun. Netw.*, vol. 4, no. 4, pp. 1048–1060, 2020.
- [23] B. Luo, P. L. Yeoh, and B. S. Krongold, "Structural properties of optimal power allocation for DAS-OFDM under joint total and individual power constraints," *IEEE Trans. Green Commun. Netw.*, pp. 1–1, 2021.
- [24] L. Liu, S. Bi, and R. Zhang, "Joint power control and fronthaul rate allocation for throughput maximization in OFDMA-based cloud radio access network," *IEEE Trans. Commun.*, vol. 63, no. 11, pp. 4097–4110, 2015.
- [25] X. Yu, W. Xu, S. Leung, X. Dang, and T. Teng, "Power allocation schemes for DAS with OFDM under per-antenna power constraint," *IEEE Trans. Veh. Technol.*, vol. 67, no. 10, pp. 10 102–10 106, 2018.
- [26] C. He, G. Y. Li, F. C. Zheng, and X. You, "Energy-efficient resource allocation in OFDM systems with distributed antennas," *IEEE Trans. Veh. Technol.*, vol. 63, no. 3, pp. 1223–1231, 2014.
- [27] X. Li, X. Ge, X. Wang, J. Cheng, and V. C. M. Leung, "Energy efficiency optimization: Joint antenna-subcarrier-power allocation in OFDM-DASs," *IEEE Trans. Wireless Commun.*, vol. 15, no. 11, pp. 7470–7483, 2016.
- [28] Z. Lin and Y. Liu, "Joint uplink and downlink transmissions in user-centric OFDMA Cloud-RAN," *IEEE Trans. Veh. Technol.*, vol. 68, no. 8, pp. 7776–7788, 2019.
- [29] Y. Dong, H. Zhang, M. J. Hossain, J. Cheng, and V. C. M. Leung, "Energy efficient resource allocation for OFDMA full duplex distributed antenna systems with energy recycling," in *Proc. IEEE Global Commun. Conf.*, 2015.
- [30] D. W. K. Ng, E. S. Lo, and R. Schober, "Energy-efficient resource allocation in OFDMA systems with large numbers of base station antennas," *IEEE Trans. Wireless Commun.*, vol. 11, no. 9, pp. 3292–3304, 2012.
- [31] S. Zhang, B. Di, L. Song, and Y. Li, "Sub-channel and power allocation for non-orthogonal multiple access relay networks with amplify-and-forward protocol," *IEEE Trans. Wireless Commun.*, vol. 16, no. 4, pp. 2249–2261, 2017.
- [32] W. Feng, N. Ge, and J. Lu, "Hierarchical transmission optimization for massively dense distributed antenna systems," *IEEE Commun. Lett.*, vol. 19, no. 4, pp. 673–676, 2015.
- [33] D. W. K. Ng, Y. Wu, and R. Schober, "Power efficient resource allocation for full-duplex radio distributed antenna networks," *IEEE Trans. Wireless Commun.*, vol. 15, no. 4, pp. 2896–2911, 2015.
- [34] D. Tse and P. Viswanath, *Fundamentals of Wireless Communication*. Cambridge, U.K.: Cambridge Univ. Press, 2005.
- [35] M. Grant and S. Boyd, "CVX: Matlab software for disciplined convex programming, version 2.2," Jan. 2020, [online] Available: <http://cvxr.com/cvx>.
- [36] *MOSEK ApS: Software for Large-scale Mathematical Optimization Problems*, version 9.2.36, Jun. 2021, [online] Available: <http://www.mosek.com>.
- [37] E. Che, H. D. Tuan, and H. H. Nguyen, "Joint optimization of cooperative beamforming and relay assignment in multi-user wireless relay networks," *IEEE Trans. Wireless Commun.*, vol. 13, no. 10, pp. 5481–5495, 2014.
- [38] H. H. Kha, H. D. Tuan, and H. H. Nguyen, "Fast global optimal power allocation in wireless networks by local D.C. programming," *IEEE Trans. Wireless Commun.*, vol. 11, no. 2, pp. 510–515, 2012.
- [39] *Evolved Universal Terrestrial Radio Access (E-UTRA) : Physical layer procedures, Release 15*, document 3GPP TS 36.213 v15.4.0, Sep. 2018.
- [40] *Universal Mobile Telecommunications System (UMTS): Spatial channel model for Multiple Input Multiple Output (MIMO) simulations, Release 16*, document 3GPP TR 25.996 v16.0.0, Dec. 2020.
- [41] *Requirements for further advancements for Evolved Universal Terrestrial Radio Access (E-UTRA) (LTE-Advanced), Release 15*, document 3GPP TR 36.913 v15.0.0, Sep. 2018.



Zhan Liu received the B.S. and M.S. degrees from Nanchang University, Nanchang, China. He is currently pursuing the Ph.D. degree with the School of Electronic and Information Engineering, South China University of Technology, Guangzhou, China. Since 2009, he has been a Researcher with the Hunan University of Humanities, Science and Technology. His research interests include Massive MIMO, full duplex wireless systems, and energy efficiency communications.



Suili Feng (M'05) received the B.S. degree in electrical engineering from South China Institute of Technology, Guangzhou, China, and the M.S. and Ph.D. degrees in electronic and communication system from South China University of Technology, Guangzhou, China, in 1982, 1989, and 1998, respectively. He was a Research Assistant with Hong Kong Polytechnic University, Hung Hom, Hong Kong, from 1991 to 1992, and a Visiting Scholar at the University of South Florida, Tampa, FL, USA, from 1998 to 1999. He has been with South China

University of Technology since 1989, where he currently works as a Professor with the School of Electronic and Information Engineering. His research interests include wireless networks, computer networks, and communication signal processing.